IOPscience iopscience.iop.org

Home Search Collections Journals About Contact us My IOPscience

GaN-based two-dimensional channels: hot-electron fluctuations and dissipation

This article has been downloaded from IOPscience. Please scroll down to see the full text article.

2009 J. Phys.: Condens. Matter 21 174203

(http://iopscience.iop.org/0953-8984/21/17/174203)

View the table of contents for this issue, or go to the journal homepage for more

Download details:
IP Address: 129.252.86.83
The article was downloaded on 29/05/2010 at 19:25

Please note that terms and conditions apply.

J. Phys.: Condens. Matter **21** (2009) 174203 (8pp) doi:10.1088/0953-8984/21/17/174203

GaN-based two-dimensional channels: hot-electron fluctuations and dissipation

A Matulionis

Semiconductor Physics Institute, A Goštauto 11, Vilnius LT-01108, Lithuania

E-mail: matulionis@pfi.lt

Received 30 September 2008
Published 1 April 2009
Online at stacks.iop.org/JPhysCM/21/174203

Abstract
Ultrafast electronic and phononic processes are investigated in voltage-biased GaN-based two-dimensional channels of interest for heterostructure field-effect transistors. The accumulation of non-equilibrium longitudinal optical phonons (hot phonons) is treated for AlGaN/GaN, AlGaN/AlN/GaN, AlGaN/GaN/AlN/GaN, and AlInN/AlN/GaN structures in terms of the hot-phonon temperature and hot-phonon lifetime. The hot-phonon effect on hot-electron energy relaxation and hot-phonon number relaxation is extracted from an experimental investigation of hot-electron fluctuations and power dissipation. The measured equivalent hot-phonon temperature is nearly equal to the hot-electron temperature. The hot-phonon lifetime varies in the range from 150 to 800 fs and depends on electron density, temperature, and supplied electric power. The experimental dependence of the hot-phonon lifetime on the hot-phonon mode occupancy is unique—neither Raman optical-photon scattering nor optical-phonon-assisted intersubband absorption has, as yet, provided any experimental data of this sort.

1. Introduction

A heterostructure field-effect transistor (HFET) is the most promising active device for microwave applications. Unprecedented power levels have been demonstrated by a GaN-based HFET with a two-dimensional electron gas (2DEG) channel [1]. Heat removal from the channel becomes the main problem. At a high power, the electrons prefer to launch longitudinal optical (LO) phonons when they dissipate their excess energy. As a result, the Joule heat is accumulated in the LO-phonon modes, and hot phonons come into play [2]. The problem of heat dissipation cannot be adequately treated without considering conversion of the hot phonons into acoustic phonons.

Hot-phonon lifetime is often introduced to treat the hot-phonon conversion [3, 4]. The lifetime has been measured for most III–V compounds [5]. The direct measurement is based on time-resolved pump–probe Raman scattering. In the Raman experiment, the scattered light is probed after hot phonons are pumped in. Intensity of anti-Stokes line decreases as the injected hot phonons gradually disappear, and the lifetime is determined from this decay. In particular, a $\sim$3 ps value is reported for GaN at room temperature [6]. The lifetime depends on ambient temperature [6] and carrier density [7]. The temperature-dependent behavior is explained in terms of the dominant Ridley mechanism [8]: an LO-phonon splits into a transverse optical (TO) and a longitudinal acoustic (LA) phonons [6, 9]. At a high density of electrons, plasmons come into play; coupled LO-phonon–plasmon modes decay faster than bare LO phonons [10]. This model [10] explains the measured dependence on the carrier density [7].

Experiments on quantum well structures have shown that the LO-phonon lifetime in normally-empty quantum wells is approximately the same as in the corresponding carrier-free bulk material [11]. On the other hand, an HFET channel usually contains a degenerate 2DEG. As mentioned, the lifetime decreases as the carrier density increases [7]. Therefore, short lifetimes can be expected in the 2DEG channels. However, the pump–probe Raman experiment is difficult to carry out on a single channel, and this technique has yielded no data on the hot-phonon lifetime in the 2DEG as yet.

The pioneering result on hot-phonon lifetime in a degenerate 2DEG was obtained from hot-electron fluctuations: a value of 350 fs was deduced for AlGaN/GaN 2DEG channel [12]. A close value of 380 fs was obtained for a similar AlGaN/GaN structure from a time-resolved pump–probe LO-phonon-assisted intersubband absorption experiment [13]. The

 © 2009 IOP Publishing Ltd Printed in the UK

fluctuation technique is applicable to 2DEG channels [14–17] and three-dimensional (3DEG) channels [18–20]. The results agree with those available from the model of coupled LO-phonon–plasmon modes [10]. The result for Si [19] is in a fair agreement with the values available from the independent response experiment [21]. The fluctuation measurements at cryogenic and elevated temperatures show a weak (if any) dependence on ambient and hot-electron temperatures [12, 22].

Monte Carlo simulation shows that hot phonons play an important role in hot-electron transport [12, 23–25] and power dissipation [26] in GaN and GaN-based 2DEG channels. The hot-phonon lifetime is the input parameter for the simulation. The electron drift velocity (at a given electric field and a given electron density) increases if the lifetime decreases [12]. The hot-phonon effect is stronger at a higher electron density [27, 28] and in degenerate 2DEG [23, 26]. The hot-phonon conversion into other vibrations is the bottleneck for power dissipation [26]. The dependences of the lifetime on electron density, temperature, and supplied power are prerequisites for physics-based 2DEG engineering.

The paper overviews the recent progress in the experimental investigation of hot-phonon lifetime in voltage-biased GaN-based 2DEG channels. The hot-electron fluctuations due to electron–LO-phonon interaction are singled out, and the hot-electron energy relaxation is considered in section 2. Section 3 deals with the fluctuation technique for estimating the hot-phonon temperature and the lifetime; the experimental dependence of the lifetime on supplied electric power and electron density is presented. The effect of hot phonons on hot-electron transport is briefly discussed in section 4. The paper ends with the summary.

2. Hot-electron fluctuations

Fluctuations originate at a microscopic level and can be used for investigation of the associated kinetic processes. The universal fluctuation-dissipation theorem states that, at thermal equilibrium, fluctuations and responses to small external perturbation carry identical information on dissipation [29]. In particular, equilibrium spectra of current and voltage fluctuations yield the electron velocity relaxation time that enters the electron low-field mobility. Electron number fluctuations contain the trapping time. Fluctuations of Faraday rotation provide the electron spin relaxation time [30]. Equilibrium phonons can be studied through fluctuations of scattered light [31]. When electrons are displaced from thermal equilibrium in a voltage-biased channel, electronic fluctuations acquire additional features, and complementary information is available [32]. Electron confinement in a 2DEG introduces specific fast and ultrafast electronic processes. The associated time constants have been extracted from hot-electron fluctuations [33–35].

It is convenient to study hot-electron fluctuations in a gateless channel supplied with two Ohmic electrodes (figure 1). An electric field is applied to heat the electrons. Short pulses of current minimize thermal walkout due to channel self-heating. The electric field agitates hot-electron velocity fluctuations, the latter induce the current fluctuations responsible for

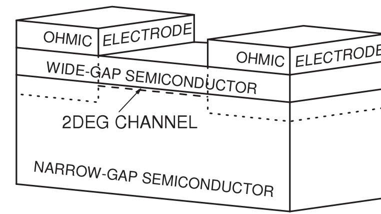

Figure 1. Schematic view of a sample supplied with two Ohmic electrodes. The 2DEG channel is located in the narrow-gap semiconductor at the heterojunction.

emission of electromagnetic radiation registered with a sensitive radiometer [34]. A typical radiometric set-up operates at a microwave frequency (say, 10 GHz) where the hot-electron fluctuations dominate while fluctuations due to electron trapping and other low-frequency sources are of negligible intensity.

The radiometer opens during the current pulse and compares the power emitted by the hot electrons with that radiated by a 'black body' kept at a known temperature. The hot-electron noise temperature equals the black-body temperature if the emitted powers are equal and the impedances match. Sample mismatch is taken into account as described elsewhere [34]. The noise power is averaged during the time domain selected in the range from 10 ns to 15 μs [16]. The time domain is delayed for measurements of the noise temperature before, during, and after the current pulse. This helps to control channel self-heating and minimize the associated thermal walkout [36].

A 2DEG channel usually forms in an undoped narrow-gap semiconductor at a heterojunction with a wide-gap semiconductor (figure 1). Selective doping is the standard technology for arsenide structures: the donors located in the wide-gap layer supply their electrons for the 2DEG. No doping is needed when the channel forms in GaN: the 2DEG originates from strong spontaneous and piezoelectric polarization [37].

In a voltage-biased 2DEG channel, an important source of hot-electron fluctuations appears when the electrons have enough energy to overcome the barriers that confine the electron gas. Reversible random jumps of electrons out of the channel and back cause channel occupancy fluctuations. The associated current fluctuations appear in the bias direction; they are often named real-space transfer (RST) fluctuations. Hot-electron RST fluctuations were resolved for the first time in the AlGaAs/GaAs single-heterojunction structure [38].

High confining barriers in GaN-based heterostructures open a wide range of electric fields where the hot-electron RST fluctuations are not important [26]. Figure 2 presents the noise temperature for two nitride structures with 2DEG channels located in the GaN layer. The RST fluctuations cause the dominant source of noise in $Al_{0.15}Ga_{0.85}N$/GaN at fields above 10 kV cm^{-1} (triangles). The conduction band offset is higher when the AlGaN alloy contains a higher Al mole ratio; correspondingly, the RST noise appears at higher electric fields. The RST fluctuations are totally suppressed when an AlN spacer is inserted between the 2DEG channel and the alloy in $Al_{0.33}Ga_{0.67}$N/AlN/GaN (squares [26]).

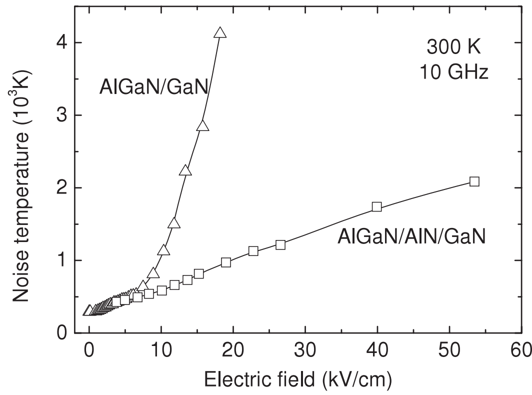

Figure 2. Dependence of hot-electron noise temperature at 10 GHz frequency for $Al_{0.15}Ga_{0.85}N/GaN$ (triangles, 5×10^{12} cm^{-2}) and $Al_{0.33}Ga_{0.67}N/AlN/GaN$ (squares, 10^{13} cm^{-2}) [26]. Solid lines guide the eye.

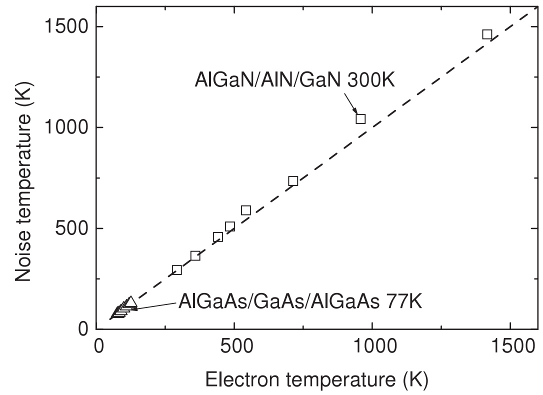

Figure 3. Calculated dependence of hot-electron noise temperature on hot-electron temperature for $Al_{0.33}Ga_{0.67}N/AlN/GaN$ (squares) [40] and AlGaAs/GaAs/AlGaAs (triangles) [41]. The dashed line is $T_{ph} = T_e$.

Hot-electron RST fluctuations can also be suppressed in another way [34]. The fluctuations manifest themselves if the channel is long and the electron transit time exceeds the RST relaxation time. As a result, the RST fluctuations are of negligible intensity in short channels; the measured dependence on the channel length yields the RST relaxation time [34]. Supposing that RST noise is suppressed, electron–phonon scattering is the main source of hot-electron fluctuations in a 2DEG channel at electric fields below the threshold for hot-electron intervalley fluctuations. Suppression of hot-electron RST fluctuations is among the goals of the 2DEG technology aimed at microwave electronics.

At a low electron density, the hot-electron energy distribution contains features at LO-phonon energy and multiples. Monte Carlo simulation shows that these features tend to disappear as the electron density increases [39]. Finally, the Fermi–Dirac distribution becomes an acceptable fit at high electric fields at the electron densities typical for GaN 2DEG channels [26]. The fitting parameter is the hot-electron temperature. It is close to the noise temperature (figure 3). This statement is approximately valid for the 2DEG channels confined in GaAs and GaN: open squares present Monte Carlo simulation data for the GaN 2DEG [40] together with those for the GaAs 2DEG (triangles) [41]. Experimental data confirm the same conclusion (figure 4): the noise temperature is close to the hot-electron temperature measured in electro-luminescence and photoluminescence experiments (horizontal bar and closed squares, respectively) [42, 43].

Open symbols in figure 4 stand for the excess hot-electron noise temperature, $T_n = T_0$, measured for the 2DEG channels in $Al_{0.82}In_{0.18}N/AlN/GaN$ (open circles) [17] and $Al_{0.33}Ga_{0.67}N/AlN/GaN$ (open squares) [46]. The excess temperature is plotted against the electric power supplied to an average electron:

$$P_s = ev_d E = UI/N_e \qquad (1)$$

where e is the elementary charge, v_d is the electron drift velocity, E is the applied electric field, U is the applied voltage, I is the current, and N_e is the number of electrons in the 2DEG channel.

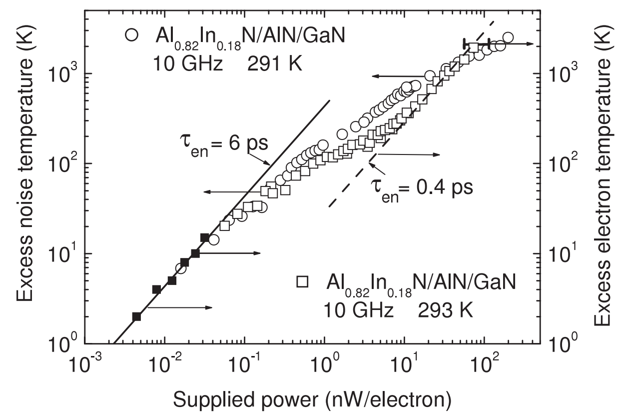

Figure 4. Dependence of excess noise temperature on supplied electric power per electron for $Al_{0.33}Ga_{0.67}N/AlN/GaN$ (squares [46]) and $Al_{0.82}In_{0.18}N/AlN/GaN$ (circles [17]). Excess hot-electron temperature is available from photoluminescence experiments on GaN (solid squares [43]) and electro-luminescence experiments on AlGaN/GaN HFET (horizontal bar [42]). Lines assume constant hot-electron energy relaxation time: $\tau_{en} = 6$ ps (solid line) and $\tau_{en} = 0.4$ ps (dashed line).

Once the hot-electron temperature is available as a function of the supplied power, the hot-electron energy relaxation time can be estimated according to:

$$\tau_{en} = k_B \frac{dT_e}{dP_s} \qquad (2)$$

where k_B is the Boltzmann constant and T_e is the electron temperature.

An almost linear increase in the hot-electron temperature is obtained at a low supplied power, $P_s < 0.1$ nW/electron (figure 4, symbols). The experimental results are close to the solid line drawn for $\tau_{en} = 6$ ps. The energy relaxation time defined after equation (2) decreases as the power increases (figure 5(a)). A sharp decrease is observed at a low supplied power. This feature means that the LO-phonon contribution to power dissipation tends to dominate

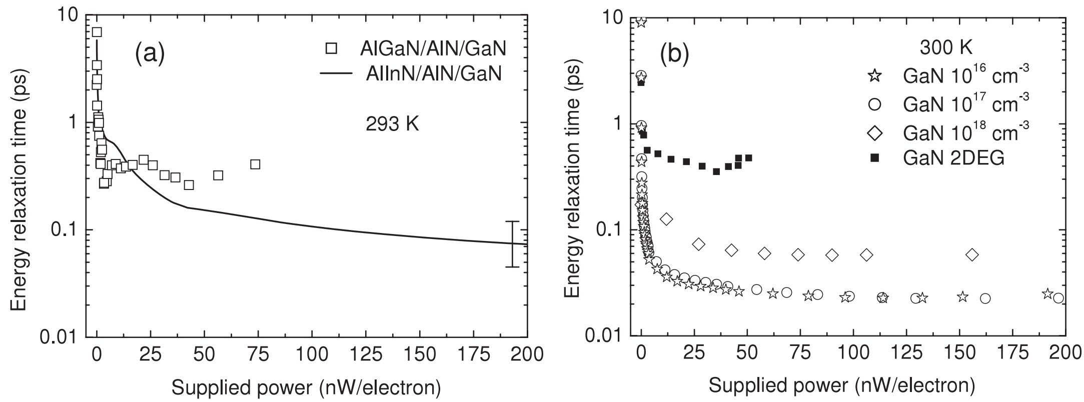

Figure 5. Hot-electron energy relaxation time after equation (2): experiment (a) and Monte Carlo simulation (b). $Al_{0.33}Ga_{0.67}N$/AlN/GaN (open squares, 1×10^{13} cm^{-2} [46]), $Al_{0.82}In_{0.18}N$/AlN/GaN (solid line, 1.2×10^{13} cm^{-2} [17]), $Al_{0.33}Ga_{0.67}N$/AlN/GaN (closed squares, $\sim 10^{20}$ cm^{-3} [26]). GaN: (stars, 10^{16} cm^{-3}), (circles, 10^{17} cm^{-3}), (diamonds, 10^{18} cm^{-3}) [39].

as the hot-electron temperature increases [46]. The transition to the LO-phonon-dominated energy relaxation follows from Monte Carlo simulation as well [26, 44].

At a high supplied power, $P_s > 10$ nW/electron, another constant value $\tau_{en} \sim 0.4$ ps (figure 4, dashed line) is reached in $Al_{0.33}Ga_{0.67}N$/AlN/GaN (open squares). For comparison, a femtosecond laser pump–probe absorption experiment yields 0.29 ps for GaN [45]. The relaxation time continues to decrease as the power increases for $Al_{0.82}In_{0.18}N$/AlN/GaN, and $\tau_{en} = 80 \pm 30$ fs is obtained at $P_s \sim 200$ nW/electron (figure 5, solid line).

The simulated hot-phonon effect on hot-electron energy relaxation time is illustrated in figure 5(b). The energy relaxation time is obtained from the simulated hot-electron temperature for $Al_{0.33}Ga_{0.67}N$/AlN/GaN [26] and from the mean kinetic energy for GaN [39]. The simulation uses a power-independent and electron-density-independent value of hot-phonon lifetime as an input parameter. The hot-phonon effect is almost negligible in GaN at low electron densities: similar values are obtained for the energy relaxation time at 10^{16} cm^{-3} (stars) and 10^{17} cm^{-3} (circles). The effect becomes essential at 10^{18} cm^{-3}: the high-power value in GaN increases from $\tau_{en} \sim 20$ fs (stars, 10^{16} cm^{-3}) to $\sim$60 fs (diamonds, 10^{18} cm^{-3}) and reaches $\sim$500 fs in the 2DEG channel (closed squares). In other words, the electron energy relaxation becomes many times slower when the hot phonons come into play.

The simulated high-power value of the hot-electron energy relaxation time (figure 5(b), closed squares) is in a reasonable agreement with the experimental data for the $Al_{0.33}Ga_{0.67}N$/AlN/GaN structure (figure 5(a), open squares). As mentioned, the simulation assumes a power-independent value for the hot-phonon lifetime. However, this assumption fails to explain the data for $Al_{0.82}In_{0.18}N$/AlN/GaN (figure 4, circles) at $P_s > 1$ nW/electron. Consequently, the hot-phonon lifetime depends on the supplied power, and this dependence can be extracted from the experimental data of figure 4.

3. Hot-phonon lifetime

3.1. Dependence on hot-phonon mode occupancy

In the electron temperature approximation, the power P_d dissipated by electrons is determined by the electron temperature and the occupancy of the involved phonon modes. For the dominant electron–LO-phonon scattering an approximate expression has been used [46]:

$$P_d = \frac{\hbar\omega}{\tau_{sp}}(1 + N_{ph})p_- - \frac{\hbar\omega}{\tau_{abs}} N_{ph} p_+ \qquad (3)$$

where $\hbar\omega$ is the LO-phonon energy, τ_{sp} is the mean time for spontaneous launching of an LO-phonon by a high-energy electron, τ_{abs} is the mean time for LO-phonon absorption, $p_\pm$ are the probabilities to find an electron able to launch (−) or absorb (+) an LO-phonon, and N_{ph} is some equivalent (average) occupancy of the hot-phonon modes. The probabilities $p_\pm$ are easily available from the Fermi–Dirac distribution and the density-of-state function [14].

The solid curve in figure 6 presents the dissipated power P_d calculated after equation (3) for a 5-subband GaN 2DEG model [46] when the equivalent hot-phonon mode occupancy is arbitrarily chosen to be $N_{ph} = 0.525$. The result is compared with the measured supplied power P_s for the $Al_{0.82}In_{0.18}N$/AlN/GaN 2DEG channel (circles). The dissipated power balances the supplied power at the crossing point where $T_e \approx 1012$ K and $P_d \approx 13$ nW/electron. Supposing that N_{ph} is expressed in degrees Kelvin, the chosen occupancy value of 0.525 is reached at 1000 K. If the equivalent hot-phonon temperature T_{ph} is introduced in this way, the obtained crossing-point hot-electron temperature $T_e \approx$ 1012 K approximately equals the assumed equivalent hot-phonon temperature $T_{ph} = 1000$ K.

In a similar way [15], one can estimate the hot-electron temperature for each arbitrarily chosen equivalent hot-phonon temperature. The procedure illustrated by figure 6 leads to the dependence $T_{ph}(T_e)$ (figure 7, circles). Similar results are obtained for the $Al_{0.33}Ga_{0.67}N$/AlN/GaN structure (bullets). The electrons interact predominately with the hot-phonon

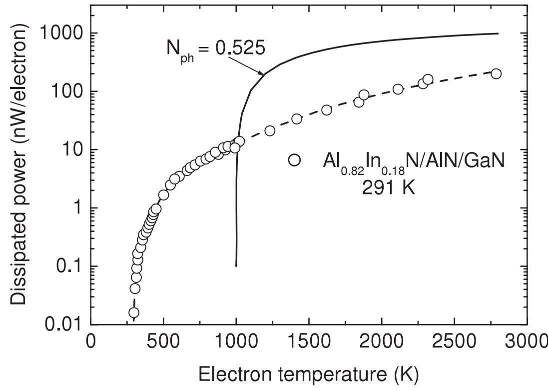

Figure 6. Measured supplied power for an $Al_{0.82}In_{0.18}N/AlN/GaN$ 2DEG channel (circles [17]) and dissipated power calculated after equation (3) for $N_{ph} = 0.525$ (solid curve). 1500 $cm^2\ V^{-1}\ s^{-1}$, $1.2 \times 10^{13}\ cm^{-2}$, 291 K. Dashed curve guides the eye.

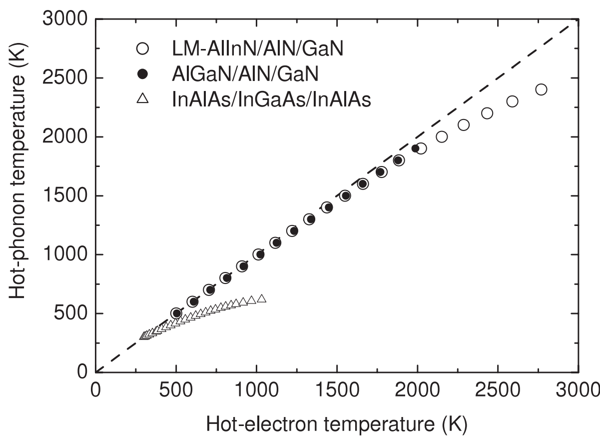

Figure 7. Dependence of equivalent hot-phonon temperature on hot-electron temperature for 2DEG channels: $Al_{0.33}Ga_{0.67}N/AlN/GaN$ (bullets [15]), $Al_{0.82}In_{0.18}N/AlN/GaN$ (open circles [17]), and AlInAs/GaInAs/AlInAs (triangles [14]). The dashed line is the hot-electron temperature.

modes selected by energy/momentum conservation. Therefore, the phonon temperature (figure 7, symbols) does not represent all phonons: it characterizes the hot-phonon modes only [15]. Indeed, acoustic phonons play a negligible role in electron energy relaxation at high electric fields [15, 17, 46].

At a hot-electron temperature of 2000 K, the hot-phonon temperature in the GaN 2DEG channels (figure 7, circles, bullets) is just several percent lower than the hot-electron temperature (dashed line). This means that the hot electrons and the hot phonons tend to form a hot subsystem where the hot particles (electrons and LO phonons) interact intensely among themselves while their coupling with the phonons beyond this subsystem is weak [12]. A similar conclusion follows from experiments on AlGaN/GaN 2DEG transistors [47]. On the other hand, a similar statement is not applicable to the 2DEG channel confined in the AlInAs/GaInAs/AlInAs heterostructure (figure 7, triangles) [14].

Open circles in figure 7 show, that the difference between the temperatures of hot electrons and hot phonons increases with the electron temperature; the difference exceeds 10% at $T_e > 2500$ K in the $Al_{0.82}In_{0.18}N/AlN/GaN$ 2DEG channel.

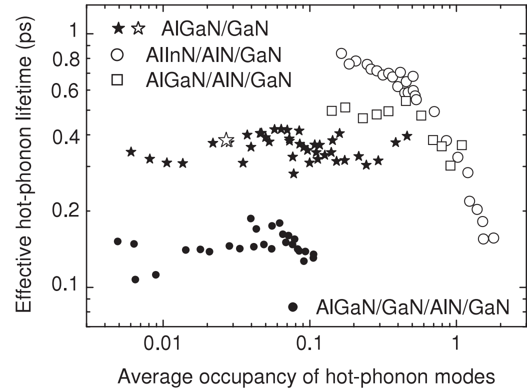

Figure 8. Dependence of effective hot-phonon lifetime on equivalent hot-phonon mode occupancy for GaN 2DEG channels: $Al_{0.15}Ga_{0.85}N/GaN$ (closed stars, $5 \times 10^{12}\ cm^{-2}$ [12, 22]), (open star [13]); $Al_{0.33}Ga_{0.67}N/AlN/GaN$ (open squares $1 \times 10^{13}\ cm^{-2}$ [15]); $Al_{0.22}Ga_{0.78}N/GaN/AlN/GaN$ (bullets, $5 \times 10^{12}\ cm^{-2}$ after [16]); $Al_{0.82}In_{0.18}N/AlN/GaN$ (open circles $1.2 \times 10^{13}\ cm^{-2}$ [17]).

Once the equivalent occupancy of the hot-phonon modes is known, the effective hot-phonon lifetime can be extracted according to [12]:

$$\tau_{ph} = \hbar\omega \frac{N_{ph} - N_0}{P_d} \quad (4)$$

where N_0 is the LO-phonon mode occupancy at equilibrium.

Under the dominant electron–LO-phonon scattering in the high-density 2DEG, the hot-phonon lifetime τ_{ph} and the hot-electron energy relaxation time τ_{en} are closely related [14, 15]:

$$\tau_{ph} = F^* \tau_\varepsilon \quad (5)$$

where the coefficient F^* is between 1.12 and 1.25 for the AlGaN/AlN/GaN 2DEG channel in the electron temperature range from 500 to 2000 K at room temperature. The relations (4) and (5) have been used for extraction of the hot-phonon lifetime from the experimental data on fluctuations in 2DEG channels [12, 14–17].

Figure 8 summarizes the experimental data on the hot-phonon lifetime for the GaN 2DEG channels. The results illustrate a weak, if any, dependence of the hot-phonon lifetime on the equivalent occupancy of the hot-phonon modes at low–moderate occupancies. In this range, the shortest lifetime of ~150 fs is obtained for the $Al_{0.22}Ga_{0.78}N/GaN/AlN/GaN$ structure (bullets) [16], the longest lifetime (~800 fs) is recorded for the $Al_{0.82}In_{0.18}N/AlN/GaN$ structure (circles) [17]. An essential dependence on the occupancy is observed for this structure (circles) when the data are taken over a wide range of supplied electric power: the lifetime decreases when the hot-phonon mode occupancy increases and tends to values below ~160 fs at $N_{ph} \sim 1.8$. None of the femtosecond time-resolved optical techniques have been applied to measure the lifetime as a function of the hot-phonon mode occupancy in a voltage-biased degenerate 2DEG of interest for microwave transistors—in this sense, the fluctuation technique remains unique.

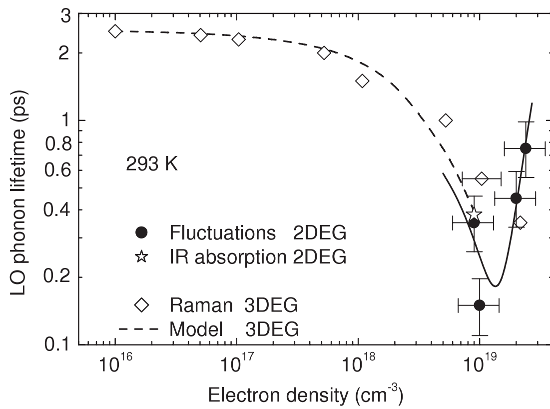

Figure 9. Dependence of hot-phonon lifetime on electron (electron–hole) density at room temperature in GaN and GaN-based 2DEG channels. Raman pump–probe data (diamonds [7]), fluctuation data of figure 8 at $N_{ph} < 0.5$ (bullets, after [12, 15–17]), intersubband absorption datum (star [13]). The dashed curve is the plasmon–LO-phonon model for GaN [10]. The solid curve is a parabolic dependence to guide the eye.

3.2. Dependence on electron density

The Raman pump–probe time-resolved technique is a direct method for experimental investigation of hot-phonon lifetime and its dependence on carrier density. According to the experimental data on bulk GaN (figure 9, diamonds), the lifetime decreases when the pump intensity increases [7] (the same conclusion follows from the results on GaAs, see [5]). This behavior is explained in terms of disintegration of coupled LO-phonon–plasmon modes (dashed curve) [10]. The available values for the GaN 2DEG channels are shown in figure 9: bullets illustrate the results extracted from hot-electron fluctuations [12, 15–17], star stands for the experiment on hot-phonon-assisted intersubband absorption [13].

The Raman data (figure 9, diamonds) are plotted against the average density of carriers per unit volume generated in bulk GaN. When the excess carriers are generated with heavily absorbed light, the generation rate decreases as the distance from the illuminated surface increases. Since the lifetime is longer at a lower density of carriers, a sharper anti-Stokes line comes from the phonons located deeper under the surface. As a result, the measured lifetime corresponds to a lower density than figure 9 shows. Supposing that the experimental points (diamonds) were shifted left, a better agreement with the dashed curve would be obtained.

The results on hot-phonon lifetime for the 2DEG channels can be compared with the Raman data on the bulk GaN when the average density per unit volume is introduced. Let it be the electron sheet density divided by the quantum well width at the Fermi energy. Since the lifetime depends on the hot-phonon mode occupancy (figure 8), the values obtained at low–moderate occupancy ($N_{ph} < 0.5$) are plotted in figure 9 (bullets). As mentioned, the shortest lifetime is reported for the $Al_{0.22}Ga_{0.78}N/GaN/AlN/GaN$ structure at the 2DEG density of $\sim 5 \times 10^{12}$ cm^{-2} [16]; this sheet density corresponds to the average density of $\sim 1 \times 10^{19}$ cm^{-3}.

At this density, the LO-phonon energy approximately equals that of the plasmon in GaN, and resonant behavior is expected. The LO-phonon–plasmon resonance means that the hot-phonon lifetime should be its shortest at around this density. The plasmon energy and the associated resonant condition are difficult to calculate for a 2DEG. However, the experimental results for the GaN 2DEG channels (figure 9, bullets) seem to confirm this expectation.

4. Hot-electron transport

Accumulation of hot phonons causes additional friction for the electron transport along the 2DEG channel. It is not straightforward to resolve the hot-phonon effect on electron drift velocity since many other scattering mechanisms act together. As mentioned, the hot-phonon effect is weak at a low density of electrons. Indeed, the electron drift velocity is high in a semi-insulating undoped GaN subjected to a high electric field. The time-of-flight experiment leads to a transient velocity value of 7.25×10^7 cm s^{-1} at 320 kV cm^{-1} [48] (recorded shortly after injection of a cloud of electrons). The transient velocity relaxes to the steady-state value of $\sim 3 \times 10^7$ cm s^{-1}. A negative differential mobility is observed at/above $\sim$300 kV cm^{-1}.

Although the time-of-flight experiment is the best for measurement of the electron drift velocity, this technique is not applicable to a 2DEG channel because of the high density of equilibrium electrons. Therefore, the electron drift velocity in 2DEG channels is often obtained either from analysis of the frequency operation of an HFET or through measurement of the current in a gateless channel [49].

The electron–phonon interaction, the hot-electron RST, and the alloy scattering cause the main friction in nominally undoped GaN-based 2DEG channels. The remote alloy scattering arises from the overlap of the free-electron wavefunctions and the random polarization and piezoelectric fields (caused by the nonuniform distribution of ions in the alloy). The overlap can be reduced if an AlN spacer is inserted between the 2DEG and the alloy layer in an AlGaN/AlN/GaN structure [50]. The additional reduction is achieved in the $Al_{0.22}Ga_{0.78}N/GaN/AlN/GaN$ structure where the AlN spacer is replaced with a thicker spacer composed of two undoped binary layers (AlN and GaN) [49]. The effect of random piezoelectric fields can be eliminated when the alloy composition is lattice-matched with the GaN layer in $Al_{0.82}In_{0.18}N/AlN/GaN$ [51]. As a result, the electron low-field mobility increases from 150 cm^2 V^{-1} s^{-1} to 1500 cm^2 V^{-1} s^{-1} in the lattice-matched $Al_{0.82}In_{0.18}N/AlN/GaN$ structure when the AlN spacer thickness increases from 0.3 to 1 nm [51].

As mentioned (see figure 2), the hot-electron RST dominates at high electric fields in the $Al_{0.15}Ga_{0.85}N/GaN$ structure [12]. The AlN spacer excludes the RST and the associated alloy scattering [17, 26]. The highest achieved mobility value is close to the calculated electron mobility caused by the equilibrium phonons only. Thus, $Al_{0.82}In_{0.18}N/AlN/GaN$ and $Al_{0.22}Ga_{0.78}N/GaN/AlN/GaN$ structures seem to be the best candidates for resolving the hot-phonon effect on electron drift velocity.

Figure 10 compares the experimental results on the electron drift velocity with those of the Monte Carlo

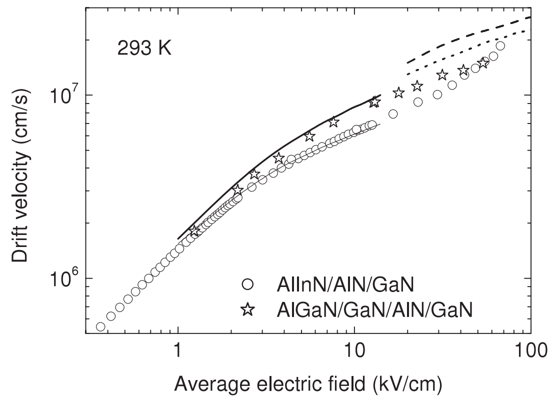

Figure 10. Dependence of electron drift velocity on electric field at room temperature for GaN-based 2DEG channels located in $Al_{0.22}Ga_{0.78}N$/GaN/AlN/GaN (stars, 5×10^{12} cm^{-2} [49]) and $Al_{0.82}In_{0.18}N$/AlN/GaN (circles, 1.2×10^{13} cm^{-2} [17]). Monte Carlo simulation (lines): no hot-phonon effect (dashes [24]), $\tau_{ph} = 0.3$ ps (dots [24]), $\tau_{ph} = 0.35$ ps (solid line [12]), $\tau_{ph} = 1$ ps (thin line [12]).

simulation. At low electric fields where the hot-phonon effect is negligible, the measured velocity (symbols) is slightly below the results of Monte Carlo simulation (solid line). This confirms that the model treats the electron–phonon scattering in an adequate way, and only weak scattering mechanisms are missing. Two independent simulations lead to close results (solid line and dots).

At moderate electric fields, the results for $Al_{0.22}Ga_{0.78}$ N/GaN/AlN/GaN (figure 10, stars [49]) remain in a fair agreement with the simulation when the hot-phonon lifetime of 350 fs is used as an input parameter (solid line [12]). At a given electron density, the hot-phonon effect is stronger if the lifetime is longer (thin line). In agreement with this statement and the long lifetime in $Al_{0.82}In_{0.18}N$/AlN/GaN at moderate occupancy of hot-phonon modes (figure 8, circles), the electron drift velocity in this 2DEG channel is lower (figure 10, circles) as compared to the data for $Al_{0.22}Ga_{0.78}N$/GaN/AlN/GaN (figure 10, stars). In addition, a higher electron density causes a stronger hot-phonon effect as well [27, 28].

The hot-phonon effect is clearly resolved at high electric fields. In the field range from 20 to 40 kV cm^{-1}, the calculated electron drift velocity for no-hot-phonon case (dashed curve) is ~80% higher than the value measured for $Al_{0.82}In_{0.18}N$/AlN/GaN (figure 10, circles). Since the hot-phonon lifetime decreases as the occupancy increases (figure 8, circles), the electron drift velocity is expected to increase with the field faster than the simulation predicts for a constant value of the lifetime. The experimental results (figure 10, circles) confirm, in part, the expectation—more efficient dissipation of the excess heat contained in the hot-phonon modes ensures better conditions for hot-electron transport.

5. Summary

Hot-electron fluctuations contain information on ultrafast electronic and phononic processes in 2DEG channels of interest for microwave electronics. The fluctuations originate where the current flows; as a result, the fluctuation techniques are applicable to 2DEG channels embedded between thick layers and/or covered with opaque coatings. The results on hot-electron energy relaxation, real-space transfer, and hot-phonon number relaxation are presented for AlGaN/GaN, AlGaN/AlN/GaN, AlGaN/GaN/AlN/GaN, and AlInN/AlN/GaN structures with the 2DEG channels located inside the GaN layer. The measured equivalent hot-phonon temperature nearly equals the hot-electron temperature. The hot-phonon lifetime in the 2DEG is essentially shorter than the value in bulk semiconductors measured at a low density of electrons. The dependence on the electron density is explained by the LO-phonon–plasmon model.

The pioneering results available from fluctuations are in good agreement with those obtained *a posteriori* by response techniques. In particular, the hot-phonon lifetime for AlGaN/GaN is close to the value extracted from subpicosecond time-resolved optical-phonon-assisted intersubband absorption experiment carried out for a similar 2DEG channel. However, the fluctuation technique demonstrates the unique application—the measurement of hot-phonon lifetime as a function of the hot-phonon mode occupancy (hot-phonon temperature)—that as yet neither Raman optical-photon scattering nor optical-phonon-assisted intersubband absorption has provided any experimental data for.

References

[1] Morkoç H 2008 *Handbook of Nitride Semiconductors and Devices* (Berlin: Springer)
[2] Kocevar P 1985 *Physica* B and C **88** 155
[3] Lugli P 1992 *Spectroscopy of Nonequilibrium Electrons and Phonons* ed C V Shank and B P Zakharchenya (Amsterdam: North-Holland) p 1
[4] Shah J 1992 *Spectroscopy of Nonequilibrium Electrons and Phonons* ed C V Shank and B P Zakharchenya (Amsterdam: North-Holland) p 57
[5] Kash J A and Tsang J C 1992 *Spectroscopy of Nonequilibrium Electrons and Phonons* ed C V Shank and B P Zakharchenya (Amsterdam: North-Holland) p 113
[6] Tsen K T, Ferry D K, Botchkarev A, Sverdlov B, Salvador A and Morkoc H 1998 *Appl. Phys. Lett.* **72** 2132
[7] Tsen K T, Kiang J G, Ferry D K and Morkoc H 2006 *Appl. Phys. Lett.* **89** 112111
[8] Ridley B K 1996 *J. Phys.: Condens. Matter* **8** L511
[9] Srivastava G P 2008 *Phys. Rev.* B **77** 155205
[10] Dyson A and Ridley B K 2008 *J. Appl. Phys.* **103** 114507
[11] Tsen K T, Joshi R P, Ferry D K and Morkoc H 1989 *Phys. Rev.* B **39** 1446
[12] Matulionis A, Liberis J, Matulionienė I, Ramonas M, Eastman L F, Shealy J R, Tilak V and Vertiatchikh A 2003 *Phys. Rev.* B **68** 035338
[13] Wang Z, Reimann K, Woerner M, Elsaesser T, Hofstetter D, Hwang J, Schaff W J and Eastman L F 2005 *Phys. Rev. Lett.* **94** 037403
[14] Aninkevičius V, Matulionis A and Matulionienė I 2005 *Semicond. Sci. Technol.* **20** 109
[15] Matulionis A 2006 *Phys. Status Solidi* a **203** 2313
[16] Šermukšnis E, Liberis J and Matulionis A 2007 *Lithuanian J. Phys.* **47** 491
[17] Matulionis A, Liberis J, Šermukšnis E, Xie J, Leach J H, Wu M and Morkoç H 2008 *Semicond. Sci. Technol.* **23** 075048

[18] Matulionis A, Liberis J, Matulionienė I, Cha H Y, Eastman L F and Spencer M G 2004 *J. Appl. Phys.* **96** 6439
[19] Liberis J, Matulionienė I, Matulionis A, Lemme M, Kurz H and Först M 2006 *Semicond. Sci. Technol.* **21** 803
[20] Liberis J, Ramonas M, Kiprijanovič O, Matulionis A, Goel N, Simon J, Wang K, Xing H and Jena D 2006 *Appl. Phys. Lett.* **89** 202117
[21] Hase M, Kitajima M, Constantinescu A M and Petek H 2003 *Nature* **426** 51
[22] Matulionis A, Liberis J, Ardaravičius L, Eastman L F, Shealy J R and Vertiatchikh A 2004 *Semicond. Sci. Technol.* **19** S421
[23] Ramonas M, Matulionis A and Rota L 2003 *Semicond. Sci. Technol.* **18** 118
[24] Barker J M, Ferry D K, Goodnick S M, Koleske D D, Allerman A and Shul R L 2004 *J. Vac. Sci. Technol.* B **22** 2045
[25] Yamakawa S, Branlard J, Saraniti M and Goodnick S M 2006 *Nonequilibrium Carrier Dynamics in Semiconductors* (*Springer Proceedings in Physics* vol 110) ed M Saraniti and U Ravaioli (Berlin: Springer) p 133
[26] Ramonas M, Matulionis A, Liberis J, Eastman L F, Chen X and Sun Y J 2005 *Phys. Rev.* B **71** 075324
[27] Ridley B K, Schaff W J and Eastman L F 2004 *J. Appl. Phys.* **96** 1499
[28] Ramonas M, Matulionis A and Eastman L F 2007 *Semicond. Sci. Technol.* **22** 875
[29] Callen H B and Welton T A 1951 *Phys. Rev.* **83** 34
[30] Oestreich M, Römer M, Haug R J and Hägele D 2005 *Phys. Rev. Lett.* **95** 216603
[31] Musha T, Borbely G and Shoji M 1990 *Phys. Rev. Lett.* **64** 2394
[32] Bareikis V, Katilius R, Pozhela J, Gantsevich S and Gurevich V 1992 *Spectroscopy of Nonequilibrium Electrons and Phonons* (*Modern Problems in Condensed Matter Sciences* vol 35) ed C V Shank and B P Zakharchenya (Amsterdam: North-Holland) p 327
[33] Matulionis A 1999 *Wiley Encyclopedia of Electrical and Electronics Engineering* vol 14, ed J G Webster (New York: Wiley) p 411
[34] Hartnagel H L, Katilius R and Matulionis A 2001 *Microwave Noise in Semiconductor Devices* (New York: Wiley)
[35] Matulionis A and Matulionienė I 2002 *Noise and Fluctuations Control in Electronic Devices* ed A A Balandin (Stevenson Ranch, CA: American Scientific Publishers) p 249
[36] Matulionis A and Liberis J 2004 *IEE Proc. Circuits Devices Syst.* **151** 148
[37] Ambacher O, Foutz B, Smart J, Shealy J R, Weimann N G, Chu K, Murphy M, Sierakowski A J, Schaff W J, Eastman L F, Dimitrov R, Mitchell A and Stutzmann M 2000 *J. Appl. Phys.* **87** 334
[38] Aninkevičius V, Bareikis V, Liberis J, Matulionis A and Kop'ev P S 1991 *Proc. 11th Int. Conf. on Noise in Physical Systems and 1/f Fluctuations* ed T Musha, S Sato and M Yamamoto (Tokyo: Ohmsha) p 183
[39] Ramonas M, Matulionis A and Eastman L F 2007 *Semicond. Sci. Technol.* **22** 875
[40] Matulionis A, Liberis J and Ramonas M 2005 *AIP Conf. Proc.* vol CP780, ed T González, J Mateos and D Pardo (New York: American Institute of Physics) p 105
[41] Lei X L and Horing N J M 1987 *Phys. Rev.* B **36** 4238
[42] Shigekawa N, Shiojima K and Suemitsu T 2002 *J. Appl. Phys.* **92** 531
[43] Wang K, Simon J, Goel N and Jena D 2006 *Appl. Phys. Lett.* **88** 022103
[44] Zubkute T and Matulionis A 2002 *Semicond. Sci. Technol.* **17** 1144
[45] Wu S, Geiser P, Jun J, Karpinski J, Wang D and Sobolewski R 2007 *J. Appl. Phys.* **101** 043701
[46] Matulionis A, Liberis J, Ramonas M, Matulionienė I, Eastman L F, Vertiatchikh A, Chen X and Sun Y J 2005 *Phys. Status Solidi* c **2** 2585
[47] Pomeroy J W, Kuball M, Uren M J and Martin T 2008 *Phys. Status Solidi* b **245** 910
[48] Wraback M, Shen H, Carrano J C, Collins C J, Campbell J C, Dupuis R D, Schurman M J and Ferguson I T 2001 *Appl. Phys. Lett.* **79** 1303
[49] Palacios T, Shen L, Keller S, Chakraborty A, Heikman S, DenBaars S P, Mishra U K, Liberis J, Kiprijanovic O and Matulionis A 2006 *Appl. Phys. Lett.* **89** 073508
[50] Smorchkova I P, Chen L, Mates T, Shen L, Heikman S, Moran B, Keller S, DenBaars S P, Speck J S and Mishra U K 2001 *J. Appl. Phys.* **90** 5196
[51] Xie J, Ni X, Wu M, Leach J H, Özgür Ü and Morkoç H 2007 *Appl. Phys. Lett.* **91** 132116